Observation of Two-Step Neutralization in Conductivity and Potentiometric Titration Curve in Polymer Grafted Charged Colloidal Systems

Priti Sundar Mohanty, Tamotsu Harada, Kozo Matsumoto, and Hideki Matsuoka*

Department of Polymer Chemistry, Kyoto University, Kyoto 615-8510, Japan

Received October 19, 2005
Revised Manuscript Received January 12, 2006

Introduction. Recently, polymer grafted charged colloidal particles have been the focus of many experimental and theoretical studies.[1−6] The stability is governed by both steric and electrostatic interactions in the polymer grafted charged colloidal system, compared with only an electrostatic interaction in a conventional charged colloidal system. Furthermore, it has been shown both theoretically[4] and experimentally[5−7] that most counterions are confined within the corona of the brushes and give rise to an effective osmotic interaction. The thickness of the brush has been shown to result from a balance of the osmotic pressure of the counterions within the brush and the configurational elasticity of the chain. At a very low salt concentration, the chains may be stretched nearly to its full length. Apart from fundamental interests, charged polymer brushes can be used to generate metallic nanoparticles within the brush layer using the confinement of gold or silver ions[8] and also be valuable in technological applications such as lubricant,[9] drug delivery,[10] and protein adsorption.[11]

A block copolymer can readily form micelles in aqueous media because of its hydrophobic and hydrophilic parts and also can be used to understand the strange adsorption behavior at the air/water interface.[14,15] However, there have been few reports on the synthesis and characterization of these particles using a block copolymer as an emulsifier by emulsion polymerization methods.

In this study, we prepared polymer grafted charged colloidal particles by the emulsion polymerization method by using poly(styrene)-*b*-poly(styrene sodium sulfonate) (PS-*b*-PSSNa) block copolymer (Figure 1) as an emulsifier. We characterized these particles by determining the surface properties by titration, hydrodynamic radius by dynamic light scattering, and core radius by atomic force microscopy. Surprisingly, we observed two equivalence points in our titration curves. Furthermore, the potentiometric titration curves were very sensitive to the salt concentration of sodium chloride (NaCl). These observations were completely contradictory to the titration of a conventional charged colloidal system without grafted chains, where one generally observes a single equivalence point. To our knowledge, there have been no such observations on the titration of polymer grafted charged colloidal systems.

Experimental Section. a. Materials. Hydrochloric acid, sodium hydroxide, 2,2′-azobis(isobutyronitrile) (AIBN), dichloromethane, methanol, and styrene were purchased from Wako Pure Chemicals (Osaka, Japan). AIBN and styrene were purified by standard methods. Trimethylsilyl iodide was purchased from Tokyo Kasei (Tokyo). Oil Orange SS was also a product of Tokyo Kasei. $CDCl_3$ and DMSO-d_6 were products of Cambridge Isotope Laboratory (U.K). Molecular sieve 4A was purchased from Wako and dried under a vacuum at 150 °C for 2 h before use. Carbon tetrachloride was dried for at least 1 h in an egg-plant flask with molecular sieves. Water used for sample preparation was ultrapure water obtained from a Milli-Q System (Millipore, Bedford, MA) whose resistance was more than 18 MΩ cm.

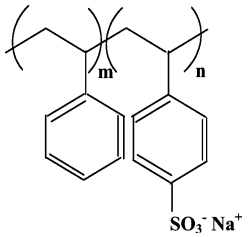

Figure 1. Chemical structure of polystyrene-*block*-poly(styrene sodium sulfonate) (PS-*b*-PSSNa) having degree of polymerization *m*:*n*. In water, PS-*b*-PSSNa dissociates in to PS-*b*-$PSSO_3^-$ and Na^+.

b. Synthesis of Block Copolymer. The block copolymer poly(styrene)-*b*-poly(styrene sodium sulfonate) (PS-*b*-PSSNa) (Figure 1) was synthesized by following the procedure reported by Okamura et al.[16] Details of synthesis have been reported elsewhere.[14a] The degrees of polymerization of PS and PSS blocks were 90 and 65, respectively. The polydispersity index (M_w/M_n) was 1.3, and the degree of sulfonation was 0.96.

c. Synthesis of Grafted Colloidal Particles. Colloidal particles of PS-*b*-PSSNa were synthesized by the emulsion polymerization method. Poly(styrene)-*b*-poly(styrene sodium sulfonate) (PS-*b*-PSSNa) block copolymer was used as an emulsifier in emulsion polymerization method.[17] Styrene as a monomer and potassium peroxodisulfate ($K_2S_2O_8$) as an initiator were used in the emulsion polymerization. The polymerization was performed for 8 h at 70 °C. The obtained suspensions of latex particles were filtered to remove the aggregates. To remove the impurities, the suspensions were passed through ion-exchange resin column and finally put in a dialysis bags for 3−4 days. The concentration of the mother suspension was determined by the dry-weight method. We synthesized two polyelectrolyte grafted PS particles, named GF1 and GF2, whose properties are summarized in Table 1.

d. Conductometric and Potentiometric Titrations. Grafted colloidal particles were ion-exchanged into the H^+ counterions from Na^+ counterions before titration. Analytical grade ion-exchange resins (Bio Rad, Richmond, CA) were used. Titrations were carried out at a temperature of 25.0 ± 0.1 °C using the conductivity meter (model DS-8M, Horiba, Japan; range = 0−100 μS/cm, frequency = 100 Hz and 100 μS/cm−100 mS/cm, frequency = 1 kHz) and the pH meter (model M-11, Horiba, Japan).

e. Dynamic Light Scattering. The hydrodynamic radius measurements were carried out using Brookhaven Instruments (Holtsville, NY). The goniometer was BI-30, and the correlator was BI-9000. The laser was NEO15-MS (Neomax, Japan) having wavelength $\lambda = 632.8$ nm.

f. Atomic Force Microscopy (AFM). The core radius was estimated by AFM using the SPI3800 probe station and the SPA300 unit system of the scanning probe microscope system SPI3800 series (Seiko Instruments, Tokyo, Japan).

Results. Conductometry and potentiometric titration were carried out with standard aqueous NaOH solution in order to determine the surface charge density of the particles. Before

* To whom correspondence should be addressed.

10.1021/ma052258l CCC: $33.50
Published on Web 02/15/2006

Table 1. Characteristics of Grafted Colloidal Suspension[a]

suspensions	charge/particle at E1 (from titration)	charge/particle at E2 (from titration)	R (E1/E2)	charge/particle (by dilution)	σ_c (nm^{-2})	R_h (nm)	D_c (nm)
GF1	2.2×10^5	6.0×10^5	36:64	1.3×10^5	0.14	88 ± 5	141
GF2	2.8×10^4	1.2×10^5	23:77	3.8×10^4	0.04	83 ± 5	128

[a] R = ratio of the charge in bulk suspension to that within the brush region, σ_c = chain density, R_h = hydrodynamic radius, and D_c= core diameter measured by AFM.

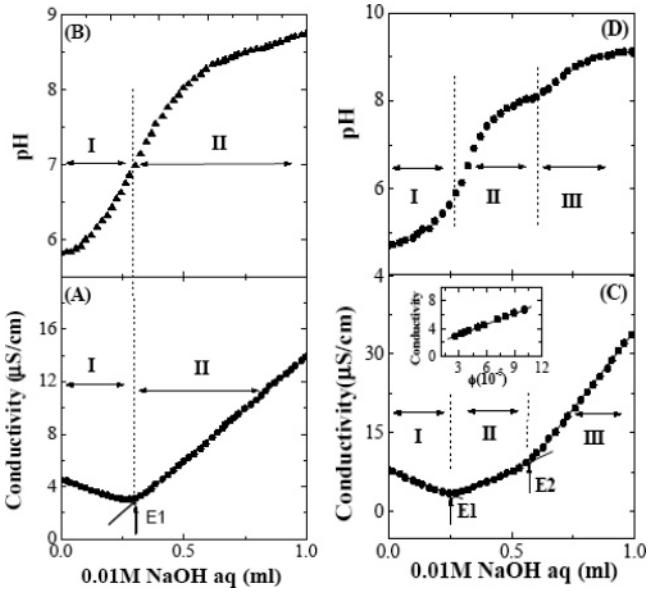

Figure 2. Conductivity and potentiometric titration curves for normal charged latex particles are shown in (A) and (B), respectively. Variations of conductivity and pH readings are plotted as a function of the titrated amount of 0.01 M NaOH. Titration was carried with a suspension having a solid content 4.0 wt %. The arrow indicates the amount of NaOH(aq) to fully neutralize sulfonic acid present in the suspension. The two solid lines in (A) are the linear fit to the conductivity data, and the intersection of the two lines is the equivalence point (denoted by the vertical arrow mark). From this equivalence point, the total number of H^+ ions per particle was estimated using the density of the polystyrene particle. Conductivity and potentiometric titration for two different synthesized grafted charged colloidal suspension. (C), (D) for GF1. The solid contents in GF1 is 0.027 wt %. The arrows indicated at E1 and E2 show that the complete neutralization occurs in two steps. The solid lines in (C) are the linear fit to the conductivity data, and the intersection point of these lines represents the equivalence points E1 and E2. Table 1 shows the charge number estimated from the two end points. The inset in (C) shows the variation of conductivity with the volume fraction of the suspension for GF1. The straight line drawn is the linear fit to the data points. From the slope of the curve, the charge number is estimated as shown in Table 1.

going to the titration of polymer grafted charged colloidal particles, we will first discuss about the typical titration curve for polystyrene charged colloidal particles of diameter 140 nm having strong sulfonic groups on its surface. Parts A and B of Figure 2 show the variation of conductivity and pH with the added amount of NaOH, respectively. The variation in conductivity curve shows two clear lines, except near the end point (shown by mark in Figure 2A). Figure 2A,B shows that the end points of the conductometry and potentiometric titration are in good agreement. These observations clearly indicate the titration of strong acid with strong base as also observed by many other groups.[18,19] From the end point, we estimated the total number of H^+ per particle to be $Z = 1500$ using the density of the polystyrene particle,1.05 g cm^{-3}.

Figure 2C,D shows conductivity and potentiometric titration curves for grafted colloidal particles (GF1) in dispersion. The titration curves are quite different; here we have observed a two-step neutralization. The conductivity curve clearly shows

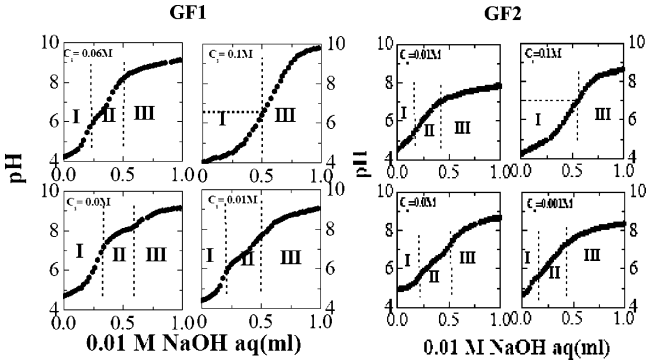

Figure 3. Potentiometric titration curves as a function of salt concentration for GF1 and GF2.

the existence of three stages (I to III). **Stage I:** Initially, the conductivity decreases as a function of NaOH concentration due to exchange of H^+ ions to Na^+ ions. This behavior is like the first step in the titration curve of a charged colloidal particles as shown in Figure 2A. This clearly shows the signature of the titration of a strong acid with strong-base. **Stage II:** In this stage, as the NaOH concentration further increases, the conductivity increases slowly. **Stage III:** In this stage, at a higher NaOH concentration, there is a further increase in the slope of the conductivity curve. The slope of the titration curve in stage III is due to the contribution from Na^+ and OH^- ions of the added NaOH. It can be noticed that the behavior of the titration curve from stage II to stage III resembles that of the titration curve of weak acid with a strong base. The three regions of the titration curves can be well fitted linearly, and the intersection of the linear fit gives two equivalence points (denoted by mark at E1 and E2). The estimated charge numbers from the first and second equivalence points and their ratios are given in Table 1. The corresponding pH curve as a function of NaOH concentration also shows three stages. But, the two equivalence points in the pH curves do not exactly match with that of the equivalence points in the counductivity curves. However, they are found to be very close to those of the observed in the conductivity titration curve. This may be due to the two different distributions of counterions inside the brush region and outside the brush region. So we have denoted with respect to three regions of the curves. This is shown in Figure 2D. Suspension GF2 also shows behavior similar to GF1 in both conductivity and potentiometric titration curves.

The inset of Figure 2C shows conductivity as a function of volume fraction (ϕ) for suspension GF1. The conductivity vs ϕ shows good linearity. The solid line is the linear fit to the conductivity data points. The intercept is identical to the value of conductivity of the deionized water (<3 μS/cm) used for the dilution. The effective charge number (H^+ ions) per particle was estimated from the slope of the curve and the equivalent conductivity of H^+ ions at infinite dilution (349.8 S cm^2 mol^{-1} at 25 °C).[20] The estimated charge number (given in Table 1) in this method is the charge, which is freely available in the suspension and plays an active role in the conductivity. The estimated charge obtained from the slope was nearly the same as that obtained from the conductivity titration curve at the first

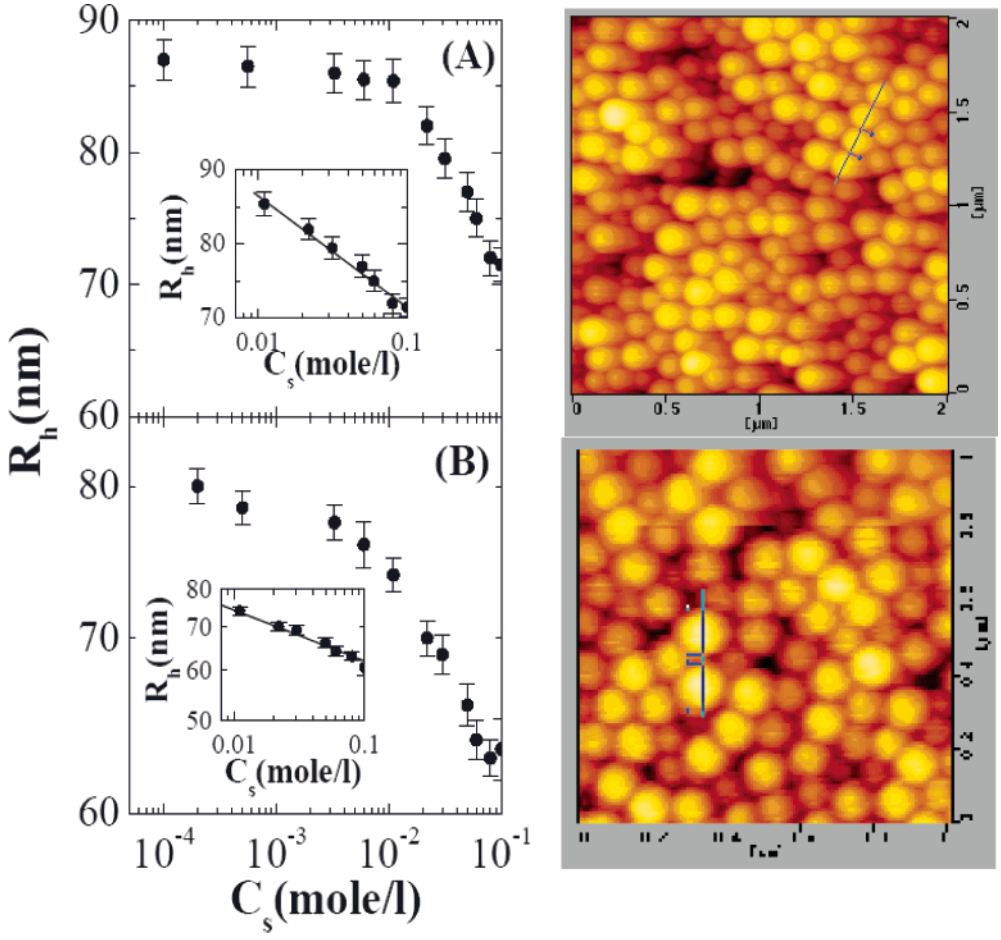

Figure 4. Hydrodynamic radius is plotted as a function of salt concentration for suspensions GF1 and GF2 in (A) and (B), respectively. The corresponding core radius measured by AFM in the dried state is shown aside.

equivalence point (marked as E1 in Figure 2C, Table 1). Suspension GF2 also showed similar behavior, and the charge number estimated is given in Table 1.

To examine the effect of added salt, we carried out potentiometric titration at different salt (NaCl) concentrations ranging from 0.0001 to 0.1 M, keeping the suspension concentrations fixed (Figure 3 for GF1 and GF2, respectively). As a function of salt concentration, the slope of the region from II to III increases rapidly. At high salt concentration, the pH curve shows only one equivalence point at around 7, which is very close to the second equivalence point of the conductivity titration curve at zero salt concentration. Hence, the second equivalence point can be regarded as the actual neutralization point for this system.

Further, the behavior of the pH curves as a function of salt concentration was further examined by measuring the hydrodynamic radius (R_h) as a function of salt concentration. The hydrodynamic radius was found to decrease after a critical salt concentration. This is shown in parts A and B of Figure 4 for GF1 and GF2, respectively. The decrease in R_h as a function of salt concentration is due to electrostatic screening of the counterions by the salt ions. In the screening region, R_h scales with the salt concentration as C_s^{α} ($\alpha = -0.1$ for GF1 and -0.08 for GF2). At high salt concentration, the R_h does not change with the further added salt concentration. Further, R_h measured at a high salt concentration is found nearly same as the radius measured by atomic force microscopy (AFM) in the dry state. The AFM image in the dried state are shown in the side of parts A and B of Figure 4 for GF1 and GF2, respectively.

Discussion. The most plausible interpretation of the present observation, i.e., "two-step neutralization", is shown in Figure 5C schematically. We should consider two kinds of counterprotons in the system, which should be different in dissociation manner. Only one possibility is ions inside and outside the ionic corona region. The counterions present in the bulk suspension are more free and expected to play an active role in the conductivity measurement. This situation cannot be achieved in conventional colloidal particles (Figure 5A), which results in one-step neutralization (Figure 5B). Since the charge estimated from the conductivity vs volume fraction was nearly equal to that of the charge number estimated from the first equivalence point, the first equivalent point (E1 shown in Figure 5D) in the titration curve corresponds to the neutralization of the $C1H^+$ counterions present in the bulk of the suspension (Figure 5C). In addition, the titration curve from stage II to stage III, which looks like the titration curve of a weak acid with strong base, suggests us the confined nature of titrated protons. Also in the case of a weak acid, the degree of dissociation varies with respect to the salt concentration. Hence in our case, we want to qualitatively tell that, though our system is a strong acid group, it behaves as a weak acid system. So it should be sensitive to the salt concentration. In fact, we have shown that the pH curves are sensitive to salt concentration. This indirectly suggest that the effective degree of dissociation changes with respect to the salt concentration. The details of the quantitative analysis is under progress. It will be reported separately. Since the slope in stage III is simply due to contribution from both Na^+ and OH^- ions, the second equiva-

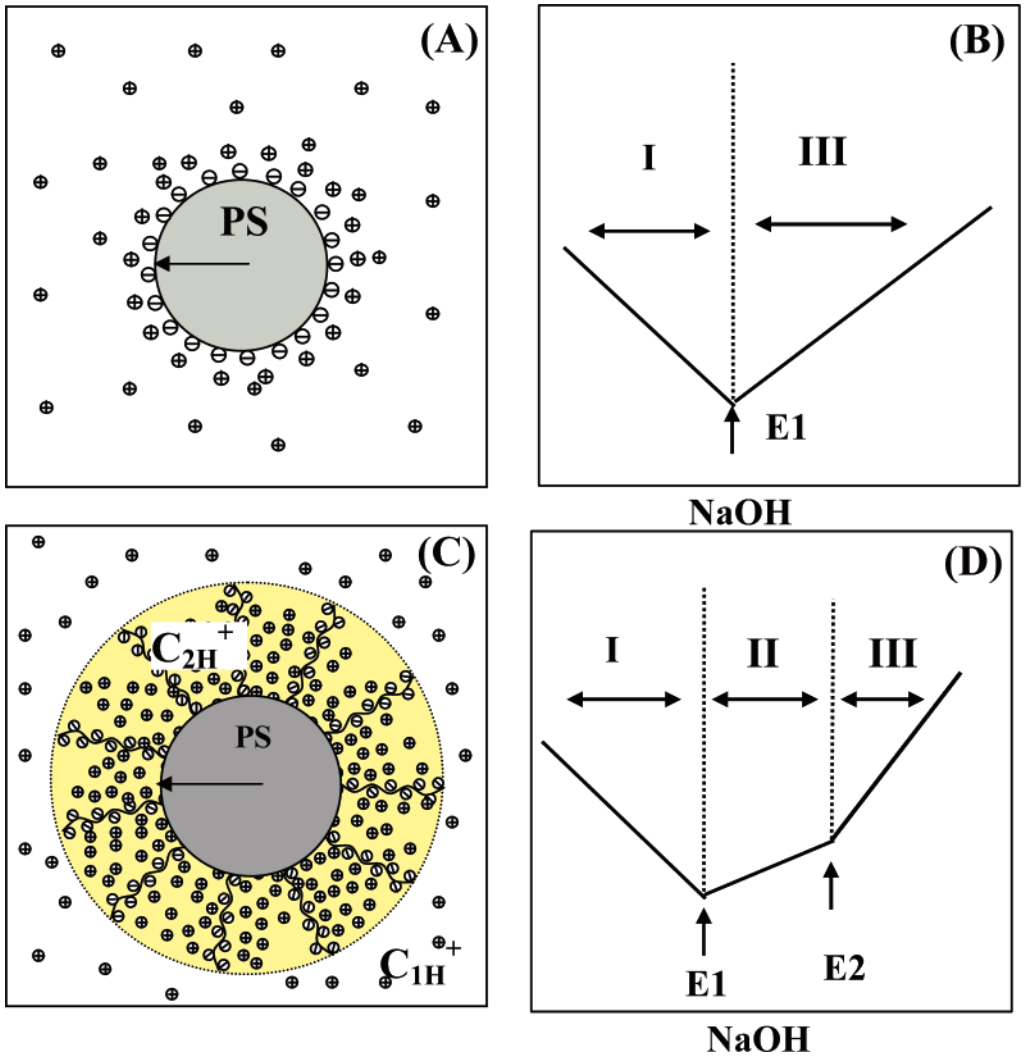

Figure 5. (A) Schematic diagram of normal charged colloidal particle. (B) The corresponding titration curve in general observed for titration of a strong acid with a strong base for normal charged colloidal particles, where one equivalence point (E1, shown by arrow) is observed. (C) Schematic diagram of polymer grafted charged colloidal particle used in the experimental study. (D) Schematic diagram of the conductivity titration curve as observed in our conductivity titration. E1 is the first equivalence point observed due to the partial neutralization of the counterions present outside the brush region (denoted by C_{1H}^+). E2 is the second equivalence point observed due to the further neutralization of excess of counterions present within the brush (yellow region denoted as C_{2H}^+). PS is the polystyrene core, and the circled − and + denote the SO^-_3 and H^+ ion, respectively.

lence point (shown in the Figure 5D) is the equivalent point of total counterprotons, which is consistent with the behavior of pH curves as a function of salt. We understood this behavior that, at high salt concentration, all the entrapped counterions release to the bulk solution. The salt ions enter within the brush region and screen the electrostatic interaction between the polymer chains. This behavior is understood by the decrease of hydrodynamic radius as a function of salt concentration.

Finally, it might be worth to note the titration behavior of other polymeric systems. Kawaguchi et al. reported two-step dissociation for linear polyelectrolytes,[21,22] which has very high charge density. This behavior was explained in the light of strong electrostatic interaction between the counterions and the charged group on the polymer chain, which greatly differ from those of the simple electrolytes in bulk solution. Essentially, counterions condensation theory[23,24] was used to explain these behaviors. Also, Kopper et al. reported multistep neutralizaion for branched polyelectrolytes,[25] which was attributed to the dissociation of ionic groups on the surface and inside the branched polymer. Our system might have a similality for both of two examples, i.e., strong electrostatic interaction and counterions confinement.

Conclusion. For the first time to be reported, we observed two equivalence points in the conductometric and potentiometric titration curves, which is in contrast to the titration curve of normal charge colloidal particles. We interpret these results with respect to the confinement of the majority of counterions within the brush regions compared to the bulk suspension. The occurrence of the first equivalence point was attributed to the neutralization of the counterions present in the bulk suspension, which was supported by results of conductivity experiment with dilution. The second neutralization point was attributed to that of counterions confined in the corona. This interpretation was supported by pH titration with salt. These results are found to be in agreement with the decrease in hydrodynamic radius, which can be clearly explained by the screening of the electrostatic interaction by the salt ions. Our new observations in conductometric and potentiometric titration will be very important in understanding the control of release of counterions from the brush region.

Acknowledgment. This work was financially supported by a grant-in-aid for Scientific Research (A15205017) from the Ministry of Education, Science, Culture, Sports and Technology

CDV

of Japan, to whom our sincere gratitude is due. This work was also supported by the 21st century COE program, COE for a United Approach to New Materials Science from the Ministry of Education, Culture, Sports, Science and Technology.

References and Notes

(1) Israels, R.; Leermakers, F. A. M.; Fleer, G. J. *Macromolecules* **1994**, *27*, 3087.
(2) Pincus, P. *Macromolecules* **1991**, *24*, 2912.
(3) Napper, D. H, *Polymeric Stabilization of Colloidal Dispersions*; Academic Press: London, 1989.
(4) Hariharan, R.; Biver, C.; Russel, W. B. *Macromolecules* **1998**, *31*, 7514, Belloni, L.; Delsanti, M.; Fontaine, P.; Muller, F.; Guenoun, P.; Mays, J. W.; Boesecke, P.; Alba, M. *J. Chem. Phys.* **2003**, *119*, 7560.
(5) Guo, X.; Ballauff, M. *Phys. Rev. E* **2001**, *64*, 051406.
(6) Wittemann, A.; Drechsler, M.; Talmon, Y.; Ballauff, M. *J. Am. Chem. Soc.* **2005**, *127*, 9688.
(7) Jusufi, A.; Likos, C. N.; Ballauff, M. N. *Colloid Polym. Sci.* **2004**, *282*, 910.
(8) Sharma, G.; Ballauff, M. *Macromol. Rapid Commun.* **2004**, *25*, 547.
(9) Raviv, U.; Giasson, S.; Kampf, N.; Gohy, J. F.; Jerome, R.; Klein, J. *Nature (London)* **2003**, *425*, 163.
(10) Constancis, A.; Meyrueix, R.; Bryson, N.; Huille, S.; Grosselin, J. M.; Gulik-Krzywicki, T.; Soula, G. *J. Colloid Interface Sci.* **1999**, *217*, 357.
(11) Wittemann, A.; Haupt, B.; Ballauff, M. *Phys. Chem. Chem. Phys.* **2003**, 1671.
(12) Gao, X.; Weiss, A.; Ballauff, M. *Macromolecules* **1999**, *32*, 6043.
(13) Rager, T.; Meyer, W. H.; Wegner, G.; Mathauer, K.; Machtle, W.; Schrof, W.; Urban, D. *Macromol. Chem. Phys.* **1999**, *200*, 1681.
(14) (a) Matsuoka, H.; Maeda, S.; Kaewasaiha, P.; Matsumoto, K. *Langmuir* **2004**, *20*, 7412. (b) Kaewsaiha, P.; Matsumoto, K.; Matsuoka, H. *Langmuir* **2005**, *21*, 9938.
(15) Matsuoka, H.; Matsutani, M.; Mouri, E.; Matsumoto, K. *Macromolecules* **2003**, *36*, 5321.
(16) Okamura, H.; Takatori, Y.; Tsunooka, M.; Shirai, M. *Polymer* **2002**, *43*, 3155.
(17) Mohanty, P. S.; Harada, T.; Matsumoto, K.; Matsuoka, H. *Polym. Prepr. Jpn.* **2005**, *45*, 1081**.**
(18) Rasmusson, M.; Wall, S. *J. Colloid Interface Sci.* **1999**, *209*, 312.
(19) Wang, C.; Nagahashi, T.; Aoki, K.; Chen, J. *J. Electroanal. Chem.* **2002**, *47*, 530.
(20) Mohanty, P. S. Ph.D. Thesis, Madras University, 2005 (unpublished).
(21) Kawaguchi, S.; Kitano, T.; Ito, K. *Macromolecules* **1991**, *24*, 6335.
(22) Kawaguchi, S.; Nishikawa, Y.; Kitano, T.; Ito, K.; Minakata, A. *Macromolecules* **1991**, *24*, 6335.
(23) Oosawa, F. *Polyelectrolyte*; Dekker: New York, 1970.
(24) Manning, G. S. *J. Chem. Phys.* **1969**, *51*, 924.
(25) Koper, G. J. M.; van Deuijvenbode, R. C.; Stam, D. D. P. W.; Steuerle, U.; Borkovec, M. *Macromolecules* **2003**, *36*, 2500.

MA052258L